Random Telegraph Signals in Proton Irradiated CCDs and APS

G. R. Hopkinson, V. Goiffon, and A. Mohammadzadeh

***Abstract*—Random telegraph dark signal fluctuations have been studied in two types of CCD and two types of CMOS active pixel sensor after proton irradiation at 1.5, 10 and 60 MeV. Time constants and activation energies were very similar, indicating a similar defect type. A large fraction of the defects are multi- rather than 2-level, suggesting a mechanism related to defect clusters being formed from initial single proton events.**

***Index Terms*—Image sensors, proton radiation effects, radiation effects, satellite applications.**

I. Introduction

RANDOM telegraph signal (RTS) fluctuations in the dark current of proton-irradiated imaging arrays (such as charge-coupled devices, CCDs and CMOS active pixel sensors, APS) have been studied by several authors (e.g., [1]–[7]). However, relatively few device types have been investigated and the nature of the lattice defects responsible for the effects remains unknown. RTS effects are important as they limit the effectiveness of on-orbit dark signal calibrations for spaceborne imaging systems and drive the need to operate the detectors at low temperatures (to reduce the dark signal fluctuations to an acceptable level).

In this study, RTS effects have been observed in two types of CCD and two types of APS. Long duration tests (up to 2 weeks for each run) have been performed at several temperatures for 'hot pixel' defects both before and after irradiation with 1.5, 10 and 60 MeV protons. These have allowed the determination of activation energies for the RTS amplitude and time constants.

It was found that RTS behavior is very similar for all devices and proton energies (and also for the pre-radiation hot pixels). With RTS occurrence probabilities of a few % per pixel, there were more multi-level defects than would be expected and most of the brightest pixels (~ 1000 per chip) were multi-level. This cannot be explained by a mechanism based on several independent collision events in a pixel (as also discussed by Nuns [3]). Hence either single RTS defects are multi-level, or several defects (each 2-level) are created by a 'single event' collision – e.g., in a cluster. In the latter case the defects cannot be dopant or impurity related as the concentrations of these are too low. Hence the defects would have to be intrinsic (due to complexes of vacancies or interstitials). RTS effects were similar at all the proton energies used, as might be expected since the fraction of displacement damage energy (NIEL) that goes into point (rather than cluster) defects is fairly constant over that range.

It was also found that a modest anneal (2 hours at ~ 50°C) decreased the number of multi-level RTS defects and turned them into 2-level defects. This may explain the lower number of multi-level defects found in [1] and [2] – which used CCDs that had been stored for ~ 1 year at room temperature.

II. Experimental

Each of the devices was mounted on a personality board and copper heatsink placed inside an evacuated chamber with a thermoelectric cooler (TEC). This allowed control of the CCD temperature to $\sim \pm 0.1$°C over the range -15°C to 20°C. The video outputs were digitized using an off-chip 16-bit ADC. A 3 MHz pixel rate was used. The CCDs were operated in inverted mode, so the surface dark current was negligible.

A. Irradiations

All irradiations were unbiased and at room temperature. Typical exposure times were $\sim$ 100 s. Masks were used to define various fluence regions (1.5 mm aluminium masks for 1.5, 9 and 10 MeV and 8 mm steel for 60 MeV) The TH7890M and STAR250 irradiations were performed in October 2002 at Ebis Iotron (now Isotron Ltd), Harwell, U.K., with 9 MeV protons. For the STAR250, 1.7 10^{10} and 1.7 10^{11} p/cm^2 regions were used for RTS testing. Although these fluences are high, the chance of getting a high dark current pixel is relatively small since the sensitive volume (the photodiode depletion region) is a small fraction of the total pixel volume. For the TH7890M, a region irradiated to $\sim 510^8$ p/cm^2 was used.

Two CCD57-10 CCDs and one STAR1000 APS were irradiated at PSI, Switzerland in November 2005. Degraders were used to reduce the beam energy to 10 and 60 MeV. The devices were irradiated as follows:

CCD57-10 # 1 10 MeV, 2.0 10^9 p/cm^2
CCD57-10 # 2 10 MeV, 1.0 10^9 p/cm^2 & 60 MeV 2.2 10^9 p/cm^2
STAR1000 #1 10 MeV, 1.0 10^{10} p/cm^2 & 60 MeV 2.2 10^{10} p/cm^2

Irradiations were also carried out in March 2006 at Ebis Iotron, Harwell at 9.0 MeV and 1.5 MeV as follows:

CCD57-10 # 1 9 MeV, 2.0 10^9 p/cm^2 and 5.0 10^8 p/cm^2
CCD57-10 # 3 10 MeV, 1.0 10^9 p/cm^2 and 3.0 10^8 p/cm^2
1.5 MeV, 1.0 10^9 p/cm^2 and 3.0 10^8 p/cm^2
STAR1000 #2 9 MeV, 1.0 10^{10} p/cm^2 and 2.0 10^9 p/cm^2
1.5 MeV, 1.0 10^{10} p/cm^2 & 2.0 10^9 10 MeV p/cm^2

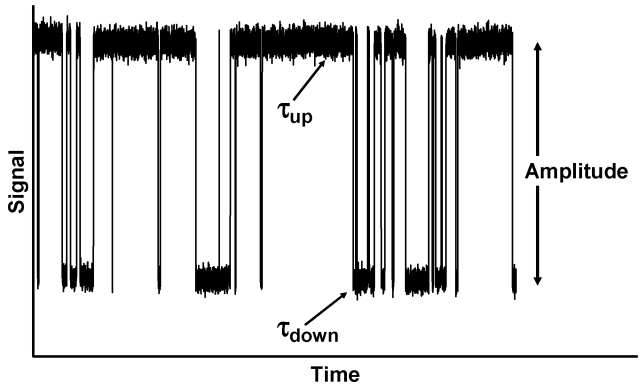

Fig. 1. Illustration of classic two-level RTS fluctuation.

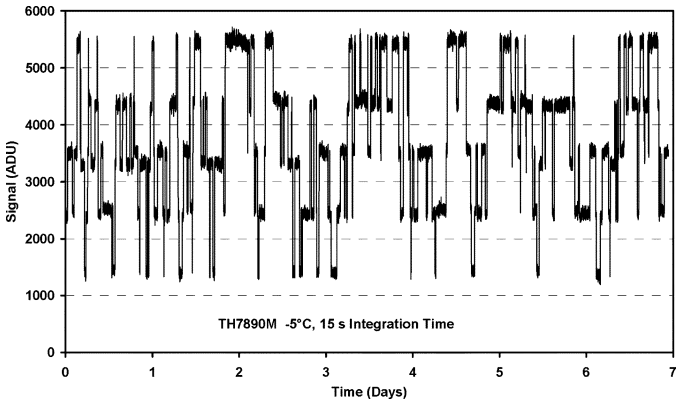

Fig. 2. Illustration of classic multi-level RTS fluctuation.

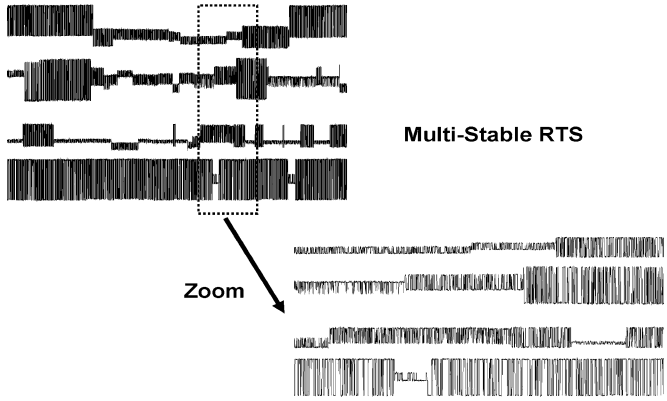

Fig. 3. Illustration of multi-bistable RTS.

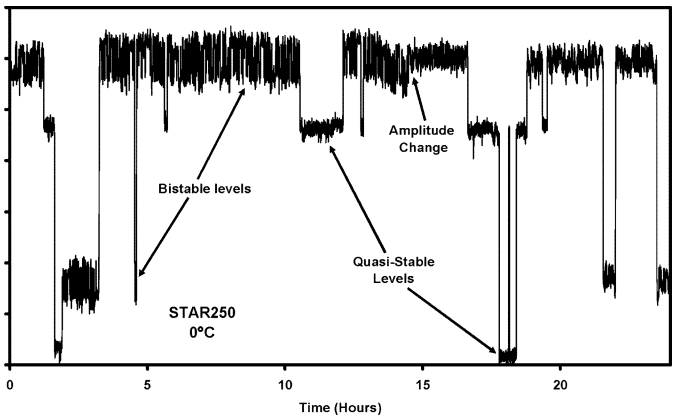

Fig. 4. Illustration of complex multi-level RTS. The term 'bistable level' refers to a level which shows fast 2-level switching. The term "quasi-stable level" refers to a level which is stable for a period of time (within which there is no switching)—but will then switch to another level.

B. Data Analysis

The RTS phenomenon results in dark current fluctuations that switch between well defined levels. In the 'classic' case of switching between two levels there are three defined parameters, as illustrated in Fig. 1. These are the:

- amplitude of the fluctuation (e.g., in electrons/pixel/s)
- average time in the high dark current state, $\tau_{\rm up}$
- average time in the low dark current state, $\tau_{\rm down}$

In fact, the classic two level fluctuation (bistable RTS) is fairly rare, even at low fluences. In general, the fluctuations are more complex; being either a superposition of several levels of fluctuation (multistable RTS) or a two level fluctuation that itself switches in amplitude and/or time constants (multi-bistable RTS)—or a mixture of the two (complex multistable or transient RTS). These more complicated RTS types are illustrated in Figs. 2–5. Many pixels will show no fluctuation (i.e., a stable level) or else a fluctuation that is erratic and appears rather like low frequency noise (probably because it has multiple levels that are not resolved in time and/or in amplitude).

For each device, data were collected for selected pixels at several temperatures. The number of pixels selected in each image varied between 1000 and 2000 and the number of images varied between 20000 (typical for TH7890M and STAR250) and 30000 (typical for CCD57 and STAR1000). The integration time (and hence the time between each image) was increased for lower operating temperatures. The integration times varied between 2 s and 60 s (the minimum time between images was 6 s) so that typical runs (30000 images) took 2–14 days. For each selected pixel the average and RMS values were calculated. RTS pixels can be identified by the anomalously high RMS value.

To analyze occurrence probabilities the pixels were selected at random. At the low fluences used, most pixels were non-RTS and had a low average dark signal level. To examine the RTS pixels in more detail, the brightest pixels in an image were selected. 2-level defects (and multi-level defects with one amplitude much larger than the others) were identified. The analysis software calculated RTS amplitudes and high and low-state time constants for 30–50 pixels in each fluence region on each device for typically 4 temperatures in the range -4°C to 18°C (in the case of one STAR1000 device, six temperatures were used in the range -15°C to 18°C). This resulted in $\sim$ 2500 analyses of 30000 data points (so more than 75 million data points). Arrhenius plots were then obtained for the amplitudes and time constants of each pixel versus inverse temperature and the activation energies calculated.

III. Results

A. Dark Current Profiles

Masking of the CCD57–10 devices into several fluence regions allows the comparison of dark signal at the three proton

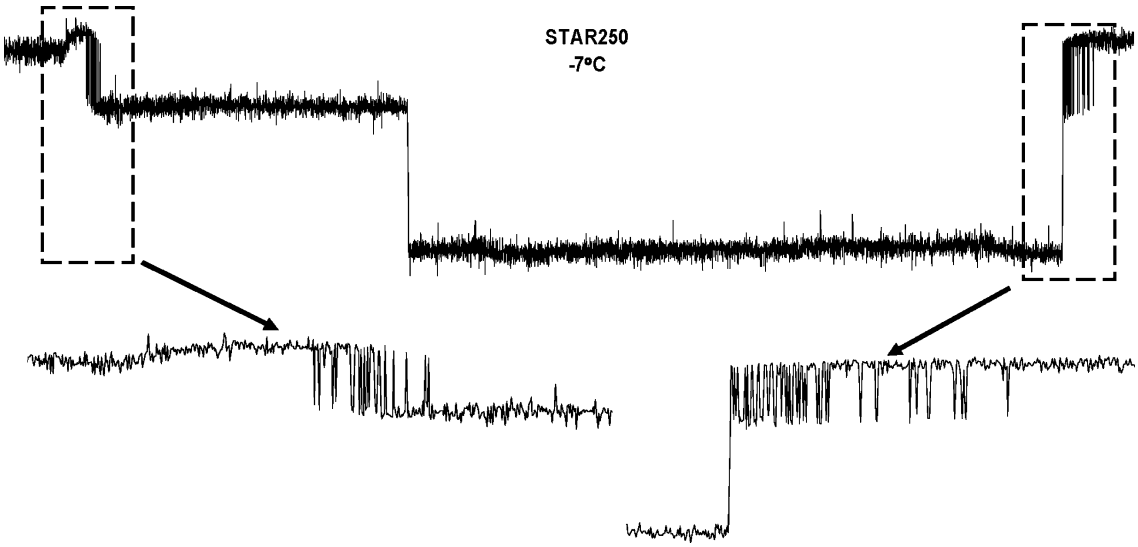

Fig. 5. Illustration of transient multi-level RTS.

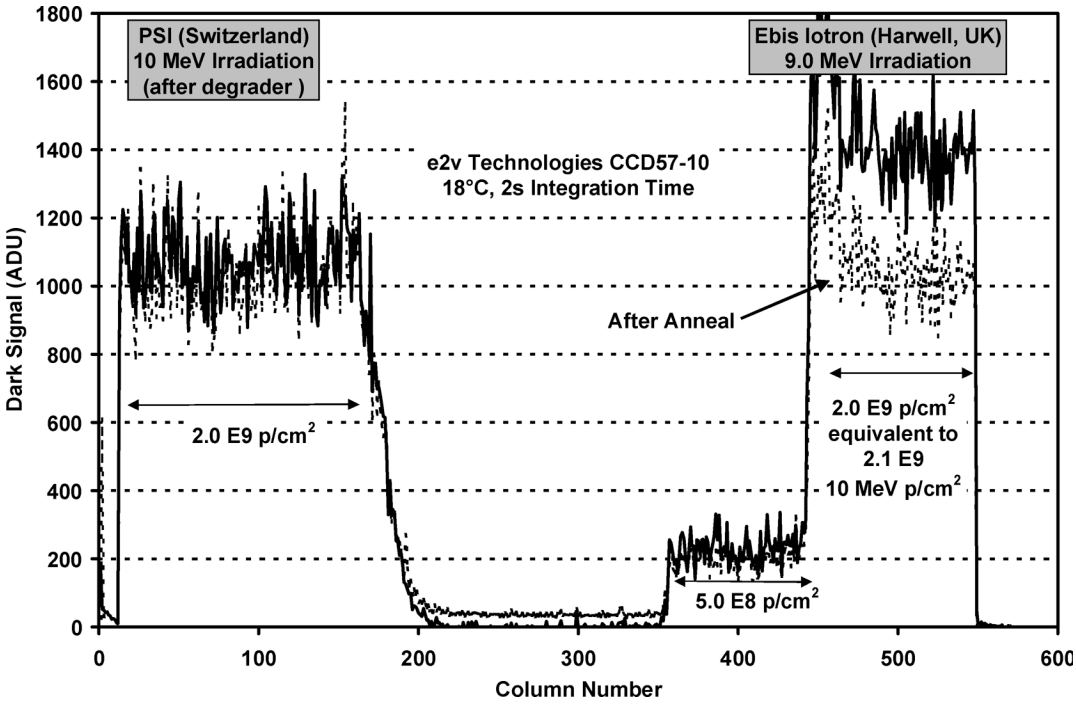

Fig. 6. Dark current profiles (average of 400 rows) across the CCD57-10 device #1 irradiated at two facilities.

energies and at the two irradiation facilities. The masks were oriented in the column direction (so each region contained ~ 100 CCD columns). Fig. 6. compares dark current data (on the same inverted-mode CCD) for irradiation at two proton facilities (obtained at room temperature with similar flux levels). The data for the PSI irradiation were taken after 4 months storage at room temperature. For the Harwell irradiations, data (shown dotted) were taken 12 days after irradiation—not long enough for defect annealing to have been fully completed. The difference in damage level is much larger than the expected $\pm 5\%$ tolerance on the measurements of proton fluence. After warming the device to $\sim 50°$C for about 2 hours, the dark current for the Harwell-irradiated CCD region annealed by a factor 1.4 and was then comparable with the PSI-irradiated region (for the same displacement damage equivalent fluence): those defects in the PSI–irradiated region that can be annealed in the temperature range up to 50°C are presumed to have been already annealed by the 4 month room temperature storage These effects illustrate the care needed to allow for post irradiation defect annealing when performing displacement damage testing. In performing a ground irradiation, the objective is to simulate the effect of the space environment, which has a relatively low average proton flux. Hence data obtained after several months room temperature annealing are most appropriate (if the CCD is operated near room temperature). However, if the CCD is to be operated significantly below room temperature, then a low temperature

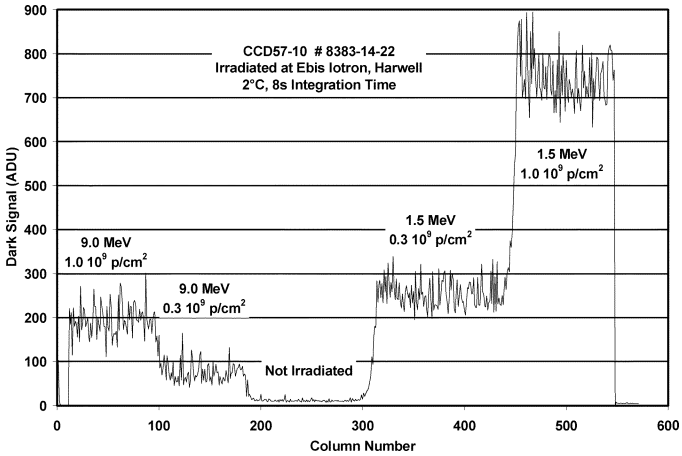

Fig. 7. Dark current profile for the CCD57-10 device #3 irradiated with 9 and 1.5 MeV protons at Harwell. Conversion gain $= 1.5$ e/ADU.

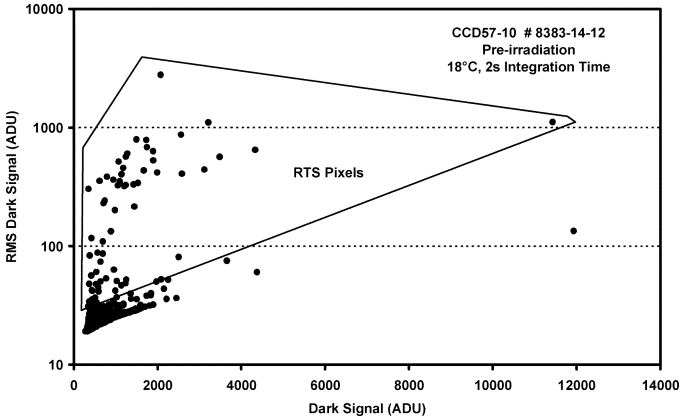

Fig. 8. RMS versus average dark current for pre-irradiation bright pixels on CCD57-10 device # 2.

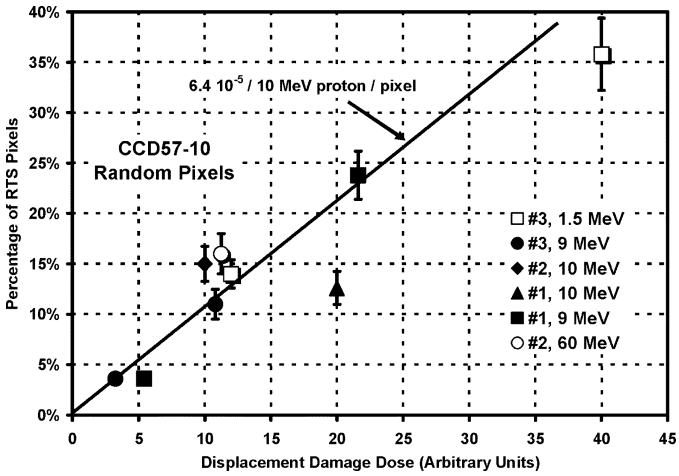

Fig. 9. Occurrence probabilities versus displacement damage dose.

irradiation is recommended (as discussed in [8] and references therein).

One of the CCD57-10 devices (#2) was proton irradiated at 10 and 60 MeV (at PSI), the higher energy having a factor 2.2 higher fluence (plot not shown). The difference in NIEL for these two energies is expected to be 2.25 [9], so that the two regions should have similar dark currents. In fact the 60 MeV region had $\sim 20\%$ higher dark current than the 10 MeV region. This is consistent with a previous study [10], where similar results were found. In the case of the 1.5 MeV protons (Fig. 7), these would be expected to have 5 times the NIEL of 9 MeV protons, whereas the experimental value is ~ 4, again indicating that higher energy protons are slightly more effective in causing dark current damage when compared to the NIEL energy dependence.

B. Occurrence Probabilities

Fig. 8 shows the RMS versus average dark current for pre-irradiation bright pixels on one of the CCD57-10 devices. Roughly one hundred RTS pixels can be identified on this and the other two CCD57-10 devices by the fact that the RMS dark signal variations are significantly increased compared with non-RTS pixels, which show only readout noise and also by checking each pixel record by eye for evidence of switching behavior (some preliminary analysis was also performed using an automated RTS detection technique, which has since been refined and is described in [11]). The similarity in the behavior of the RTS pixels (amplitudes, time constants and activation energies) to proton-induced RTS pixels suggests that the defects are the same (or similar) and may also be radiation-induced. For example, they may have been produced during manufacture by processes such as ion-implantation. It is common for ion-implantation damage to be annealed out by heat treatments during manufacture, but in this case some of the defects may not have been fully annealed. Dark current defects can be generated by cosmic rays from the terrestrial environment (see, for example [12]). However, the CCDs were only manufactured a few months previously and did not undergo any air transport before pre-irradiation testing, hence this is an unlikely cause. For the STAR1000, the number of pre-irradiation defects was much smaller (1–3 per device). The TH7890M and Star250 were not studied pre-irradiation.

Fig. 9 shows the occurrence probabilities for RTS defects after proton irradiation (both 2- and multi-level) obtained from analysis of blocks of 500 random pixels in each fluence region of each device (again identified by their large RMS fluctuations and by visually checking each pixel record). It is seen that the probabilities scale well with displacement damage dose (DDD). In particular the probabilities are similar at both 1.5 and 60 MeV (after allowing for the difference in DDD). The only data point that is significantly anomalous is the 10 MeV PSI irradiation (2×10^9 p/cm^2) for device #1. The reason for the low number of RTS pixels (63, rather than an expected number roughly twice as large) is not known but perhaps some un-intentional annealing occurred (without our knowledge) during the 4 months storage between the PSI and Harwell irradiations.

In Fig. 9, the displacement damage dose is derived from the total non-ionizing energy loss, NIEL, (i.e., the sum of elastic and non-elastic components). In an earlier work [2] it was suggested that RTS probability might scale with elastic NIEL (which is the same as total NIEL for proton energies of a few MeV but reduces to $\sim 90\%$ of the total at 10 MeV and $\sim 60\%$ at 60 MeV [9]). This was suggested because hot pixels are likely to be produced by 'common' events that happen (rarely) to occur in high field

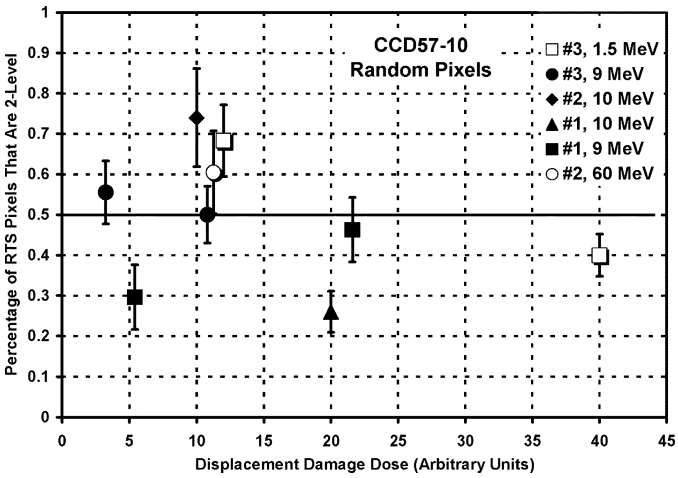

Fig. 10. Ratio of the number of 2-level RTS pixels to the total number of RTS pixels for CCD57-10 devices at various proton energies.

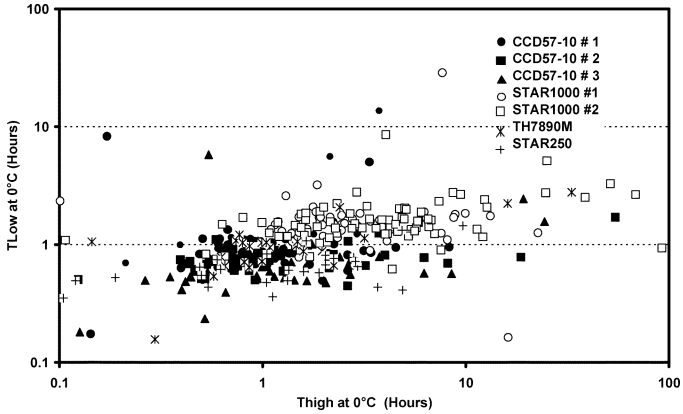

Fig. 11. Time constants for the high and low states at 0C (for RTS pixels), both are $\sim$ 1 hour for most pixels but there is more spread in the high-state times.

regions of the device. However (and to some extent with the earlier study also), even though a large number of pixels were studied, the statistics are not good enough to determine whether the probabilities scale with total or elastic NIEL—though, in this case, the fit is slightly better for the total NIEL hypothesis. (See also the discussion in [6], which came to a similar conclusion.) What can be said with some certainty, is that the probability for RTS pixels does not scale with inelastic NIEL (otherwise the probability at 1.5 MeV would be very small). NIEL scaling is an important subject since it has a bearing on the identification of the collision mechanisms responsible for RTS defects. However, given the lack of clear evidence for total versus elastic scaling, it is better to turn to the probabilities for 2- level compared with multi-level defects to gain further insight into defect mechanisms.

For the randomly selected pixels, roughly 50% of the RTS pixels were 2-level, regardless of fluence or proton energy. This can be seen in Fig. 10 (combined with Fig. 9 which gives the probability for all RTS pixels). This data does not agree with what would be expected for a Poisson distribution, $\mathrm{p}(\mathrm{n},\lambda)$, of the form:

$$\mathrm{p}(\mathrm{n},\lambda) = \mathrm{p}(\mathrm{n},\lambda)^{\mathrm{n}}\frac{\mathrm{e}^{-\lambda}}{\mathrm{n!}} \qquad (1)$$

where n is the number of defects in a pixel and λ is the proton fluence multiplied by the probability of getting a 2-level RTS defect. For example, at a fluence of 10^9 10 MeV $\mathrm{p/cm^2}$ the data indicates that about 5% of random pixels show 2-level RTS (actually this will be an upper limit since measurements at greater signal to noise ratio or carried out for longer times might show that pixels are actually multi-level). This means that only 0.1% of pixels should have more than one 2-level defect (hence being multi-level).

The fact that there are a significant number of multilevel defects even at low fluences (and low RTS occurrence probabilities) suggests that either:

- A significant fraction of individual RTS defects are multi-level (multi-stable defects), or
- Defects are (predominantly) 2-level, but the 'collision events' that create the RTS defects give defects that are clustered closely together, with several occurring in an RTS pixel.

Note that this must also be true at both 1.5 and 60 MeV proton energy—even though we expect collisions with 1.5 MeV protons to give predominantly point, rather than cluster, defects (see also the discussion in Section IV). This conclusion is also borne out by results obtained from the brightest pixels (typically the brightest 1–2% in each fluence region)—where it was found that the majority ($\sim 80-90\%$) of RTS pixels were multi-level (the majority of bright pixels: $\sim 90\%$ for the CCD57-10 and $\sim 60\%$ for the STAR1000 showed RTS of some kind).

After an 'unintended' 2 hour 50°C anneal of device 8383-14-09 the percentage of 2-level fluctuations rose from $\sim 20\%$ to approximately 50%, indicating some re-structuring (either of the individual defects or of the 'clusters', depending on the mechanism). The fact that annealing gives a smaller fraction of multi-level defects may explain the fact that early studies—which were on devices irradiated several years previously—showed few multi-level defects.

Annealing studies have also been carried out for the TH7890M and CCD57-10. There was a significant reduction in RTS pixels after storage for 3 days at 83°C which continued after a further 3 days at 110°C. Almost all had annealed after a further 3 days at 150°C.

C. Time Constants and Activation Energies

As mentioned in Section II-B, time constants and activation energies were measured for 30–50 pixels 2-level pixels in each fluence region on each device for typically 4 temperatures in the range -4°C to 18°C (for one STAR1000 device, six temperatures were used in the range -15°C to 18°C). The results are shown in Figs. 11 and 12. There is a remarkable consistency between devices and proton energies—suggesting a common defect. A few % of RTS pixels can show either very short or very long time constants or time constants that are very dissimilar (i.e., most time being spent in either the high or the low state). RTS time constants can, in fact, vary by up to 4 orders of magnitude: seconds to hours at room temperature, but the majority

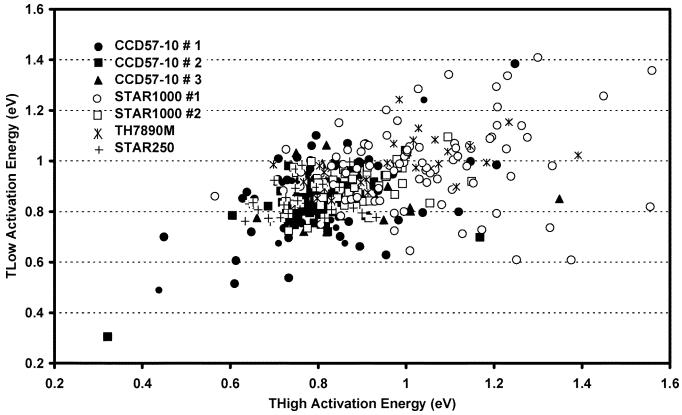

Fig. 12. Activation energies for the time constants, most values are in the range 0.8–1 eV for all devices.

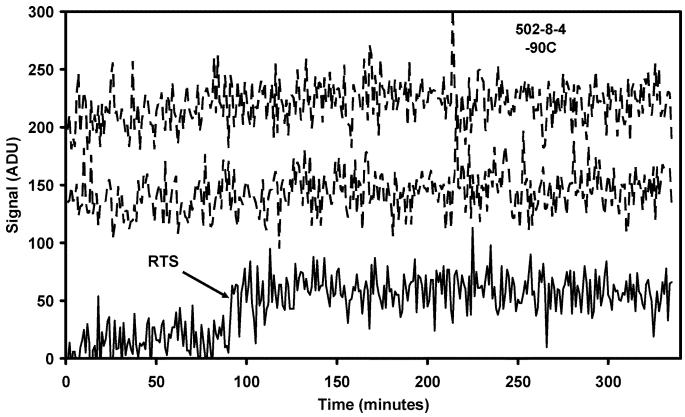

Fig. 13. Plots for two 'typical' pixels (dashed) from a CCD42–40 device at $-90°$C that showed no switching effects and for the one pixel (solid) where a transition was identified.

of RTS pixels show time constants on the order of a few hours at 0°C (i.e., minutes at room temperature).

The time constant activation energies for the APS devices were found to be similar (~ 0.9 eV) to the CCDs and to results from most previous studies (e.g., [1] and [2])—but differ from those of Boegaerts *et al.* [6] (who found a value of 0.6 eV). The reason for this discrepancy is unknown but may be linked to their operation in 'soft reset' mode which shows image lag effects, whereas this study used a reduced pixel bias to achieve 'hard reset' (cf. [13] for further discussion).

Note that the activation energies for amplitudes and time constants relate to different physical mechanisms. The amplitude activation energy relates to the change in dark current generation with temperature has a mid-gap value (though slightly decreased due to the field enhancement effect). The activation energy for the RTS time constants relates to the energy barrier encountered when a defect switches between different structural configurations.

Assuming a time constant of 1 hour at 0°C, with an activation energy of 0.9 eV, we can a predict an average time constant of ~ 5000 hours at $-50°$C. However, it has previously been seen that RTS fluctuations can be observed at low temperatures (even as low as $-90°$C, cf. Fig. 13). The fact that RTS is observable at low temperatures (on timescales of a few hours) may be due to

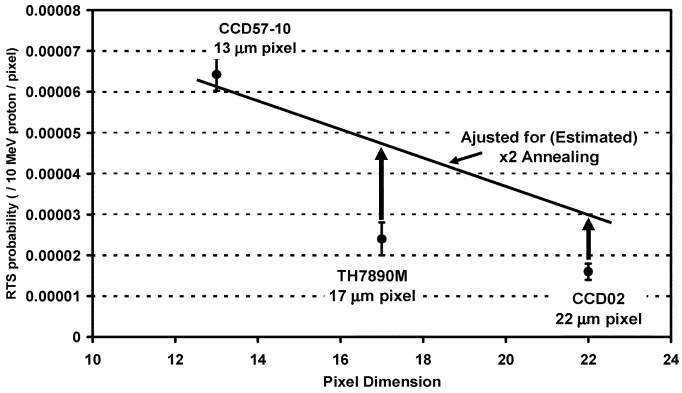

Fig. 14. Suggested RTS model allowing for factor 2 annealing for TH7890M and CCD02 data.

rare pixels that have very short time constants near room temperature (and so are not observable)—but become noticeable at low temperatures when the time constants are increased.

IV. Summary and Discussion

A. Prediction of RTS Effects

RTS occurrence probabilities, amplitudes, time constants and their activation energies have been studied for CCD57-10 and TH7890M CCDs and STAR250 and STAR1000 APS. Effects in all these devices were very similar indicating a single defect type and the possibility to make general predictions for the appearance of RTS fluctuations.

Time constants and their activation energies are shown in Figs. 11 and 12. Fig. 9 showed the occurrence probability for RTS pixels versus displacement damage dose. It seems reasonable to assume (based on this and previously published data) that occurrence probability is proportional to displacement damage dose (DDD)—at least, there is no strong evidence that it does not scale with DDD. The data suggests an occurrence probability of $6.4\ 10^{-5}$/10 MeV equivalent proton/pixel for the CD57-10. It is to be expected that CCDs with a small pixel area will have a relatively large part of their volume that has a high electric field (the high field region tends to be concentrated at the edges of the channel stops). Fig. 14 shows the results for the TH7890M and CCD57-10, together with previous data for the CCD02. However both the TH7890M and CCD02 data are for devices irradiated a year or more previously. We assume (somewhat arbitrarily) that this results in a factor ~ 2 annealing and the data has been appropriately corrected. This shows a scaling with the pixel dimension and it is suggested that this model is used for RTS predictions, at least as a first approximation.

The RTS probability is $\sim 10^{-10}$/(10 MeV proton/cm^2) for these CCDs. For the STAR1000 devices the occurrence probability is much lower (presumably because of the small volume of the photodiodes compared with the pixel pitch). The photodiodes have approximately 2.6 μm$\times$ 2.6 μm area [14] and there are four in each pixel). Given the small numbers of RTS pixels in the 500 pixel blocks studied, an estimate of occurrence probability is not very accurate for the APS devices—but if we assume ~ 10 RTS pixels are created in 500 pixels at a fluence of $1\ 10^{10}$ 10 Mev p/cm^2, then we get an occurrence probability of

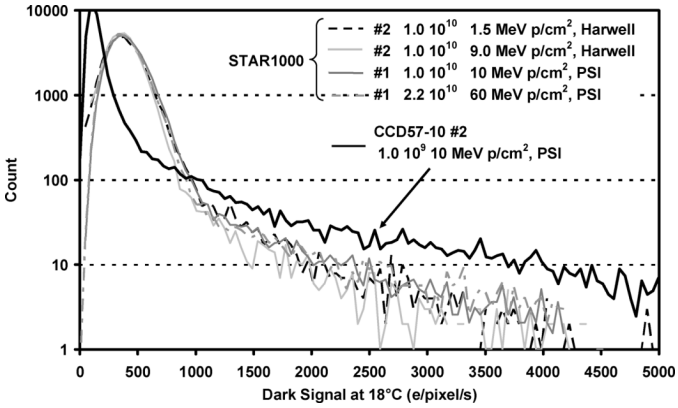

Fig. 15. Dark signal histograms for proton irradiated CCD57-10 and STAR1000 devices.

$\sim 910^{-7}/10$ MeV p/pixel, i.e., a factor 50 below that for a CCD. This factor is roughly the same order of magnitude as the ratio in pixel dimension (there will not be an exact scaling because of differences in doping and depletion depth).

The amplitude of the RTS fluctuations will tend to follow the histogram of dark signal values—since RTS amplitudes are typically 10–50% of the total pixel brightness. For the CCD57-10 and STAR1000 typical RTS amplitude will be $\sim$ 200 electrons/pixel/s at 0°C but can be a factor 5 higher. Dark signal histograms (for the whole pixel brightness, not just the RTS part) are shown in Fig. 15. The activation energies for dark signal were typically in the range 0.5–0.65 eV as expected (field enhancement lowers the activation energy below the 'normal' value of $\sim$ 0.65 eV). Note that the number of 'hot' pixels for the STAR1000 devices was small and the poor statistics may explain why the 1.5 MeV histogram (in Fig. 15) shows fewer high dark current pixels than expected (the histogram is similar to the 9 and 10 MeV plots, which have the same fluence but lower NIEL)—other explanations may be dosimetry errors or annealing effects.

B. Defect Mechanisms

For freshly irradiated devices, at most 50% of the RTS pixels were 2-level, regardless of fluence or proton energy. This strongly argues against the hypothesis that multi-level defects are due to several 2-level defects (from independent collision events) occurring in the same pixel (which would result in a Poisson distribution with very low numbers of multi-level defects). Hence, either a multi-level defect is involved—or else several 2-level defects are created (e.g., in a cluster) by single collision events. It is difficult to draw definite conclusions on microscopic defect mechanisms from what are macroscopic (device-level) measurements—and previous discussions (referenced above) have only given tentative models. However, it is speculated, based on current evidence (including the annealing behavior that changes multi- to 2-level fluctuations at temperatures $\sim$ 50°C), that the latter (cluster) explanation is more plausible. Whatever defect is responsible, it is produced by 1.5 MeV protons as well as at higher energies. At first glance it might be thought that this argues against a cluster hypothesis (at low proton energies most of the collision events are elastic and generate only low energy primary knock-on atoms, PKAs, and hence only point defects, not clusters). However, although the collision events that generate cluster defects are rare at 1.5 MeV, they contribute a significant fraction of the non-ionizing energy loss (and hence the number of dark current defects) and this fraction does not change much over the range up to 60 MeV (cf. Beck *et al.* [15] and Srour and Palko [16]).

TABLE I

Device	Format	Manufacturer
TH7890M	512 x 512, 17 μm x 17 μm pixels	e2v (formerly Atmel) Grenoble, France
CCD57-10	512 x 512, 13 μm x 13 μm pixels	e2v Technologies, Chelmsford, UK
STAR250	512 x 512, 25 μm x 25 μm pixels	Cypress Semiconductor Belgium
STAR1000	1024 x 1024, 15 μm x 15 μm pixels	Cypress Semiconductor Belgium

It would be interesting to study RTS effects in an electron irradiated device (e.g., using low energy, around 1–5 MeV), which would give only point defects (and no clusters). Formation of small vacancy clusters might still be possible by diffusion and association of isolated vacancies, though this is unlikely. Hence RTS pixels might be expected to be rare in electron irradiated devices. It would be interesting to study this in future work.

Gill *et al.* [17] have proposed clustered divacancies as an explanation for enhanced dark signal (via charge exchange reactions) but there was no suggestion of switching behavior. Defects that are bistable (i.e., have more than stable state and can reversibly pass from one to the other) have been reviewed by Mukashev [18]. Many have too shallow an energy level (for efficient dark signal generation) or require unlikely impurity levels and so are not likely to give an explanation. Dopant-vacancy complexes do appear to have the necessary multiple potential wells in the defect configuration diagram [19] and the phosphorous-vacancy pair (E center) has the necessary energy barrier of 0.9 eV [20], however this defect is inconsistent with the clustering hypothesis for multi-level RTS discussed above. A mechanism involving the single divacancy is also unlikely as its annealing temperature is too high. For similar reasons, the VO-complex defect suggested by Umeda [21] seems unlikely in our devices. Higher order vacancy complexes or some kind of interaction of the vacancy-type defects within a cluster is not ruled out however (for example, Kozlowski [22] have proposed that the trivacancy is responsible for a mid-gap level at 0.545 eV below the conduction band). Cluster defects have also been discussed in [23]–[26]. These papers indicate that small vacancy-clusters are responsible for defects with energy levels in the range 0.42–0.45 eV below the conduction band. Note that field enhanced emission will shift the energy level at which peak emission takes place from mid-gap to lower energies (see, for example, [19])—hence defects around 0.44 eV can be efficient dark current generators.

Based on the above evidence, it is tentatively concluded that RTS defects are most likely to be associated with vacancy-related defect clusters, however this identification is by no means certain and further work will be needed to confirm this hypothesis.

ACKNOWLEDGMENT

The authors would like to thank R. Brun and W. Hajdas (PSI), and R. Sharp and K. Jones (Isotron) for their assistance with the irradiations.

REFERENCES

[1] I. H. Hopkins and G. R. Hopkinson, "Random telegraph signals from proton-irradiated CCDs," *IEEE Trans. Nucl. Sci.*, vol. 40, no. 6, pp. 1567–1574, Dec. 1993.

[2] I. H. Hopkins and G. R. Hopkinson, "Further measurements of random telegraph signals in proton-irradiated CCDs," *IEEE Trans. Nucl. Sci.*, vol. 42, no. 6, pp. 2074–2081, Dec. 1995.

[3] T. Nuns, G. Quadri, J.-P. David, O. Gilard, and N. Boudou, "Measurements of random telegraph signal in CCDs irradiated with protons and neutrons," *IEEE Trans. Nucl. Sci.*, vol. 53, no. 4, pp. 1764–1771, Aug. 2006.

[4] T. Nuns, G. Quadri, J.-P. David, and O. Gilard, "Annealing of proton-induced random telegraph signal in CCDs," *IEEE Trans. Nucl. Sci.*, vol. 54, no. 4, pp. 1120–1128, Aug. 2007.

[5] A. M. Chugg, R. Jones, M. J. Moutrie, J. R. Armstrong, D. B. S. King, and N. Moreau, "Single particle dark current spikes induced in CCDs by high energy neutrons," *IEEE Trans. Nucl. Sci.*, vol. 50, no. 6, pp. 2011–2017, Dec. 2003.

[6] J. Boegaerts, B. Dierickx, and R. Mertens, "Random telegraph signals in a radiation-hardened CMOS active pixel sensor," *IEEE Trans. Nucl. Sci.*, vol. 49, no. 1, pp. 249–257, Feb. 2002.

[7] D. R. Smith, A. D. Holland, and I. B. Hutchinson, "Random telegraph signals in charge coupled devices," *Nucl. Instrum. Methods Phys. Res. A*, vol. 530, pp. 521–535, 2004.

[8] G. R. Hopkinson and A. Mohammadzadeh, "Low temperature alpha particle irradiation of a STAR1000 CMOS APS," *IEEE Trans. Nucl. Sci.*, vol. 55, no. 4, pp. XXX–XXX, Aug. 2008.

[9] C. J. Dale, L. Chen, P. J. McNulty, P. W. Marshall, and E. A. Burke, "A comparison of Monte Carlo and analytical treatments of displacement damage in Si microvolumes," *IEEE Trans. Nucl. Sci.*, vol. 41, no. 6, pp. 1974–1983, Dec. 1994.

[10] G. R. Hopkinson and A. Mohammadzadeh, "Comparison of CCD damage due to 10 and 60 MeV protons," *IEEE Trans. Nucl. Sci.*, vol. 50, no. 6, pp. 1960–1967, Dec. 2003.

[11] V. Goiffon, P. Magnan, G. Hopkinson, and L. Boucher, *A Method for Automated Random Telegraph Signal Detection and Characterization in Image Sensors*, submitted for publication.

[12] A. J. P. Theuwissen, "Influence of terrestrial cosmic rays on the reliability of CCD image sensors-part I: Experiments at room temperature," *IEEE Trans. Electron Dev.*, vol. 54, no. 12, pp. 3260–3266, Dec. 2007.

[13] G. R. Hopkinson, A. Mohammadzadeh, and R. Harboe-Sorenson, "Radiation effects in a radiation tolerant CMOS active pixel sensor," *IEEE Trans. Nucl. Sci.*, vol. 51, no. 5, pp. 2753–2762, Oct. 2004.

[14] G. Meynants, B. DierickX, and D. Scheffer, "CMOS active pixel image sensor with CCD performance," *Proc SPIE*, vol. 3410, pp. 68–76, 1998.

[15] M. J. Beck, L. Tsetseris, M. Caussanel, R. D. Schrimpf, D. M. Fleetwood, and S. T. Pantelides, "Atomic-scale mechanisms for low-NIEL dopant-type dependent damage in Si," *IEEE Trans. Nucl. Sci.*, vol. 53, no. 6, pp. 3621–3626, Dec. 2006.

[16] J. R. Srour and J. W. Palko, "A framework for understanding displacement damage mechanisms in irradiated silicon devices," *IEEE Trans. Nucl. Sci.*, vol. 53, no. 6, pp. 3610–3620, Dec. 2006.

[17] K. Gill, G. Hall, and B. MacEvoy, "Bulk damage effects in irradiated silicon detectors due to clustered divacancies," *J. Appl. Phys.*, vol. 82, no. 1, pp. 126–136, Jul. 1997.

[18] B. N. Mukashev, K. A. Abdullin, and Y. V. Gorelkinskii, "Metastable and bistable defects in silicon," *Physics-Uspekhi*, vol. 43, no. 2, pp. 139–150, 2000.

[19] J. S. Nelson, P. A. Schultz, and A. F. Wright, "Valence and atomic size dependent exchange barriers in vacancy-mediated dopant diffusion," *App. Phys. Lett.*, vol. 73, no. 2, pp. 247–249, Jul. 1998.

[20] M. G. Ganchenkova, V. A. Borodin, and R. M. Nieminem, "Annealing of vacancy complexes in P-doped silicon," *Nucl. Instrum. Meth Phys. Res. B*, vol. 228, pp. 218–225, 2005.

[21] T. Umeda, K. Okonogi, S. Tsukada, K. Hamada, S. Fujieda, and Y. Mochizuki, "Single silicon vacancy-oxygen complex defect and variable retention time phenomenon in dynamic random access memories," *Appl. Phys. Lett.*, vol. 88, pp. 243504-1–243504-3, 2006.

[22] R. Kozlowski, P. Kaminski, E. Nossarzewska-Orlowski, E. Fretwurst, G. Lindstroem, and M. Pawlowski, "Effect of proton fluence on point defect formation in epitaxial silicon for radiation detectors," *Nucl. Instrum. Meth Phys. Res. A*, vol. 552, pp. 71–76, 2005.

[23] R. M. Fleming, C. H. Seager, D. V. Lang, P. J. Cooper, E. Bielejec, and J. M. Campbell, "Effects of clustering on the properties of defects in neutron irradiated silicon," *J. Appl. Phys.*, vol. 102, pp. 043711-1–043711-13, 2007.

[24] P. F. Ermolov, D. E. Karmanov, A. K. Leflat, V. M. Manankov, M. M. Merkin, and E. K. Shabalina, "Neutron-irradiation-induced effects caused by divacancy clusters with a tetravacancy core in float-zone silicon," *Semiconductors*, vol. 36, no. 10, pp. 1114–1122, 2002.

[25] I. Kovacevic, V. P. Markevich, I. D. Hawkins, B. Pivac, and A. R. Peaker, "Vacancy-related complexes in neutron-irradiated silicon," *J. Phys. Condens. Matter*, vol. 17, pp. S2229–S2235, 2005.

[26] M. Ahmed, S. J. Watts, J. Matheson, and A. Holmes-Seidle, "Deep-level transient spectroscopy of silicon detectors after 24 GeV proton irradiation and 1 MeV neutron irradiation," *Nucl. Instrum. Meth. Phys. Res., A*, vol. 457, pp. 588–594, 2001.